Macromolecules

Article

pubs.acs.org/Macromolecules

Synthesis of Novel Optically Active Poly(phenyleneethynylene−aryleneethynylene)s Bearing Hydroxy Groups. Examination of the Chiroptical Properties and Conjugation Length

Hiromitsu Sogawa,[†,∥] Yu Miyagi,[†] Masashi Shiotsuki,[‡] and Fumio Sanda*[,§]

[†]Department of Polymer Chemistry, Graduate School of Engineering, Kyoto University, Katsura Campus, Nishikyo-ku, Kyoto 615-8510, Japan

[‡]Molecular Engineering Institute, Kinki University, Kayanomori, Iizuka, Fukuoka 820-8555, Japan

[§]Department of Chemistry and Materials Engineering, Faculty of Chemistry, Materials and Bioengineering, Kansai University, 3-3-35 Yamate-cho, Suita, Osaka 564-8680, Japan

Supporting Information

ABSTRACT: Novel optically active poly(phenyleneethynylene-aryleneethynylene)s bearing hydroxy groups with various arylene units [poly(**1**−**2**), poly(**1**−**3a**), poly(**1**−**3b**), poly(**1**−**4**)] were synthesized by the Sonogashira−Hagihara coupling polymerization of (*S*)-3,5-diiodo-4-hydroxy-$C_6H_4CONHCH(CH_3)COOC_{12}H_{25}$ (**1**) with HC≡C−Ar−C≡CH [**2** (Ar = 1,4-phenylene), **3a** (Ar = 2,7-naphthylene), **3b** (Ar = 1,4-naphthylene) and **4** (Ar = 1,6-pyrenylene), and the optical properties were compared. Polymers with number-average molecular weights (M_n) of 5,300−11,300 were obtained in 88−94% yields. CD and UV−vis spectroscopic analysis revealed that all the polymers formed predominantly one-handed helical structures in THF. The order of absorption maxima (λ_{max}) of the polymers was poly(**1**−**3a**) < poly(**1**−**2**) < poly(**1**−**3b**) < poly(**1**−**4**). Poly(**1**−**2**), poly(**1**−**3a**), poly(**1**−**3b**), and poly(**1**−**4**) emitted blue, purplish blue, green and yellow fluorescence, respectively.

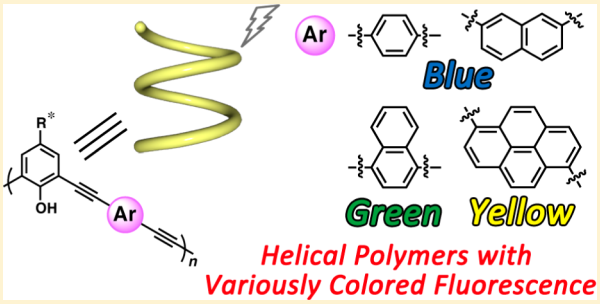

INTRODUCTION

Conjugated polymers with regulated higher order structures show useful properties including molecular recognition, chiral catalysis and chemical sensing together with electronic and optical properties.[1] Poly(phenyleneethynylene) is a typical conjugated polymer that features photoelectric properties, photoluminescence, and electroluminescence. The conjugation length of the polymer backbone largely affects the absorption and luminescent properties.[2] Poly(phenyleneethynylene)s have a nature to adopt a folded helical conformation. *m*-Linked oligo(phenyleneethynylene)s bearing tetraethylene glycol moieties at the side chains are folded into helices in polar solvents such as acetonitrile/water based on the amphiphilicity originating from the hydrophilic side chains and hydrophobic main chains.[3] Many efforts have been made to synthesize such helical phenyleneethynylene polymers, and to investigate the chiroptical properties.[4−20] We have recently revealed that D-hydroxyphenylglycine- and L-tyrosine-derived poly(*m*-phenyleneethynylene-*p*-phenyleneethynylene)s form helically folded structures due to π-stacking between phenylene moieties, intramolecular hydrogen bonding between the amide groups at the side chains, and amphiphilicity caused by hydrophobic exterior (alkyl groups and phenyleneethynylene main chain) and hydrophilic interior (hydroxy groups).[21−25] It is noteworthy that the amphiphilic balance of our polymers is opposite from that of typical helically folded poly(*m*-phenyleneethynylene) derivatives reported so far.

Naphthalene[26,27] and pyrene[28,29] are flat-shaped aromatic molecules that gather much interest because of their photoelectric functions. Extension of conjugation length is expected by introducing these condensed aromatic rings into the main chains of π-conjugated polymers, when the aromatics are linked at proper positions.[30−35] For instance, 1,4-naphthylene and 1,6-pyrenylene linkages are effective for this purpose,[31,32,34,35] while 2,7-naphthylene linkage is not because of its kinked structure and inefficient resonance.[33] There are several reports on the synthesis of π-conjugated polymers containing pyrene moieties at the main chains,[33−36] and also optically active helical polymers containing pyrene moieties at the side chains.[37−41] Nevertheless, there is no report concerning chiral conjugated polymers containing pyrene moieties at the main chains as far as we know.

There are many reports regarding the change of conjugation length of helical polymers in response to external stimuli and/or additives.[42−45] On the other hand, there are only a few examples that control the conjugation length of helical

Received: August 19, 2013
Revised: October 19, 2013
Published: November 4, 2013

Scheme 1. Sonogashira−Hagihara Coupling Polymerization of Diiodophenylene Monomer 1 with Diethynylarylene Monomers 2, 3a, 3b, and 4

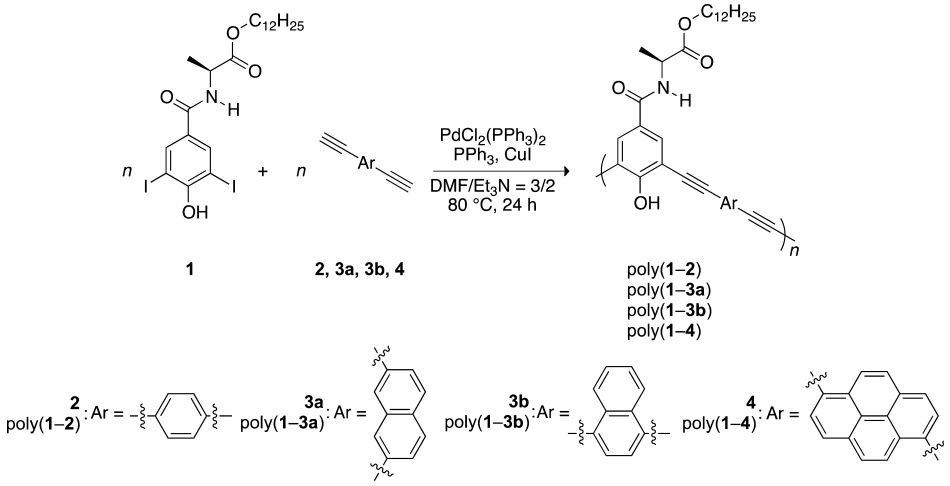

polymers by adjusting the conjugation of monomer repeating units.[46−48] Herein we report the synthesis of novel optically active poly(phenyleneethynylene−phenyleneethynylene) poly(**1**−**2**), poly(phenyleneethynylene−napthyleneethynylene)s poly(**1**−**3a**) and poly(**1**−**3b**), and poly(pheyleneethynylene−pyrenyleneethynylene) poly(**1**−**4**) containing hydroxy groups by the Sonogashira−Hagihara coupling polymerization of the corresponding monomers (Scheme 1). This paper discusses the effects of phenylene, naphthylene, and pyrenylene units on the chiroptical and fluorescence properties, conjugation length of the polymers, and secondary structures based on DFT calculations as well as CD, UV−vis, and fluorescence spectroscopic analysis.

EXPERIMENTAL SECTION

Measurements. Proton (400 MHz) and Carbon-13 (100 MHz) NMR spectra were recorded on a JEOL EX-400 or a JEOL AL-400 spectrometer. IR spectra were measured on a JASCO FT/IR-4100 spectrophotometer. Melting points (mp) were measured on a Yanaco micro melting point apparatus. Mass spectra were measured on a JEOL JMS-MS700 mass spectrometer. Specific rotations ($[\alpha]_D$) were measured on a JASCO DIP-1000 digital polarimeter. Number- and weight-average molecular weights (M_n and M_w) of polymers were determined by size exclusion chromatography (SEC, Shodex columns KF805 × 3) eluted with tetrahydrofuran (THF) calibrated by polystyrene standards at 40 °C. CD and UV−vis absorption spectra were recorded on a JASCO J-820 spectropolarimeter, and fluorescence spectra were recorded on a FP-750 spectrometer.

Materials. Unless stated otherwise, reagents and solvents were purchased and used without purification. 4-[4,6-Dimethoxy-1,3,5-triazin-2-yl]-4-methylmorpholinium chloride (TRIAZIMOCH) and trimethylsilylacetylene were provided as gifts from Tokuyama Co., Ltd. and Shin-Etsu Chemical Co., Ltd., respectively. 2,7-Diethynylnaphthalene (**3a**)[49] and 1,4-diethynylnaphthalene (**3b**)[50] were synthesized according to the literature reports. Et_3N and *N*,*N*-dimethylformamide (DMF) used for polymerization were distilled prior to use.

Monomer Synthesis. *N*-*tert*-Butoxycarbonyl-L-alanine Dodecyl Ester. 1-Ethyl-3-(3-dimethylaminopropyl)carbodiimide hydrochloride (EDC•HCl, 11.5 g, 60.0 mmol), 4-dimethylaminopyridine (DMAP) (0.732 g, 6.00 mmol), and 1-dodecanol (11.2 g, 60.0 mmol) were added to a solution of *N*-*tert*-butoxycarbonyl-L-alanine (9.45 g, 50.0 mmol) in CH_2Cl_2 (80 mL) at 0 °C, and the resulting mixture was stirred at room temperature overnight. It was washed with 0.5 M HCl, saturated $NaHCO_3$ aq., and saturated NaCl aq., dried over anhydrous $MgSO_4$, and then filtered to afford *N*-*tert*-butoxycarbonyl-L-alanine dodecyl ester in quantitative yield. The product was used in the next step without purification. ^{1}H NMR (400 MHz, $CDCl_3$): δ 0.88 (t, J = 7.2 Hz, 3H, $-CH_2CH_3$), 1.23−1.41 [m, 21H, $-OCH_2(CH_2)_9-$, $-CH_3$], 1.44 [s, 9H, $-C(CH_3)_3$], 1.63−1.65 (m, 2H, $-CH_2CH_3$), 4.06−4.18 [m, 2H, $-OCH_2(CH_2)_9-$], 4.26−4.29 (m, 1H, $-CH-$), 5.31 (br, 1H, $-NH-$). ^{13}C NMR (100 MHz, $CDCl_3$): δ 13.76 ($-CH_2CH_2CH_3$), 18.21 ($-CH_3$), 22.39 ($-CH_2CH_2CH_3$), 25.54 ($-CH_2CH_2CH_3$), 27.99 [$-C(CH_3)_3$], 28.94, 29.06, 29.22, 29.28, 29.34, 29.36, 29.40 [$-(CH_2)_7-$], 31.63 ($-OCH_2CH_2-$), 53.12 ($-CH-$), 62.31 ($-OCH_2CH_2-$), 79.18 [$-C(CH_3)_3$], 163.18 [$-COOC(CH_3)_3$], 173.11 ($-COOCH_2-$).

Dodecyl (*S*)-2-(4-Hydroxy-3,5-diiodobenzamido)propanoate (1). Trifluoroacetic acid (TFA, 10 mL, 135 mmol) was added to a solution of *N*-*tert*-butoxycarbonyl-L-alanine dodecyl ester (13.2 g, 35.5 mmol) in THF (15 mL) at 0 °C, and the resulting mixture was stirred at room temperature overnight. The resulting solution was concentrated in vacuo to obtain L-alanine dodecyl ester trifluoroacetate salt as a viscous liquid. Et_3N (7.00 mL, 50.2 mmol) was added to a solution of L-alanine dodecyl ester trifluoroacetate salt (3.71 g, 10.0 mmol) in THF, and then the resulting mixture was stirred at room temperature for 2 h. 4-Hydroxy-3,5-diiodobenzoic acid (3.89 g, 10.0 mmol) and TRIAZIMOCH (3.24 g, 10.0 mmol) were added to the solution subsequently, and the resulting mixture was stirred at room temperature overnight. It was washed with 1.0 M HCl, saturated $NaHCO_3$ aq., and saturated NaCl aq., dried over anhydrous $MgSO_4$, and then filtered. The filtrate was concentrated, and the residual mass was purified by silica gel column chromatography eluted with $CHCl_3$/hexane =4/1 (v/v), followed by recrystallization to obtain dodecyl (*S*)-2-(4-hydroxy-3,5-diiodobenzamido)propanoate as a white solid in 26%. Mp 104−105 °C. $[\alpha]_D$ +14° (c = 0.10 g·dL^{-1}, THF). IR (KBr): 3445, 3058, 2918, 1740, 1625, 1537, 1447, 1389, 1349, 1315, 1173, 1127, 765, 703 cm^{-1}. ^{1}H NMR (400 MHz, $CDCl_3$): δ 0.88 (t, J = 7.2 Hz, 3H, $-CH_2CH_3$), 1.23−1.52 [m, 21H, $-OCH_2(CH_2)_9-$, $-CH_3$], 1.63−1.65 (m, 2H, $-CH_2CH_3$), 4.14−4.20 [m, 2H, $-OCH_2(CH_2)_9-$], 4.71−4.75 (m, 1H, $-CH-$), 6.05 (br, 1H, $-NH-$), 6.58 (s, 1H, $-OH$), 8.12 (s, 2H, Ar). ^{13}C NMR (100 MHz, $CDCl_3$): δ 14.04 ($-CH_2CH_2CH_3$), 18.34 ($-CH_3$), 22.58 ($-CH_2CH_2CH_3$), 25.72 ($-CH_2CH_2CH_3$), 28.43, 29.10, 29.24, 29.28, 29.40, 29.46, 29.52 [$-(CH_2)_7-$], 31.81 ($-OCH_2CH_2-$), 48.61 ($-CH-$), 65.87 ($-OCH_2CH_2-$), 82.11, 129.48, 138.39, 156.39 (Ar), 163.44, ($-NHCO-$), 173.39 ($-COOCH_2-$). Anal. Calcd for $C_{22}H_{33}I_2NO_4$: C, 41.99; H, 5.29; N, 2.23. Found: C, 41.71; H, 5.28; N, 2.19.

1,6-Diethynylpyrene (4). 1,6-Dibromopyrene (2.16 g, 6.00 mmol), $Pd(PPh_3)_2Cl_2$ (0.213 g, 0.60 mmol), PPh_3 (0.314 g, 2.40 mmol), and CuI (0.342 g, 3.60 mmol) were fed into a two-neck flask, ant it was flushed with dry nitrogen. THF (40 mL) and Et_3N (15 mL) were added to the solution, and then trimethylsilylacetylene (4.20 mL, 30.0 mmol) was added dropwise to the solution. The mixture was

dx.doi.org/10.1021/ma401730e | Macromolecules 2013, 46, 8896−8904

stirred at 50 °C for 72 h. The resulting mixture was concentrated in vacuo and the residual mass was washed with Et_2O to extract the product. The organic phase was washed with 1.0 M HCl, and saturated NaCl aq., dried over anhydrous $MgSO_4$, and then filtered. The filtrate was concentrated, and the residual mass was purified by silica gel column chromatography eluted with hexane/EtOAc = 9/1 (v/v) and subsequently by preparative HPLC (eluent $CHCl_3$) to obtain 1,6-bis(trimethylsilylethynyl)pyrene. After that, it was dissolved in $CHCl_3$ (60 mL), and then a suspension of K_2CO_3 (2.76 g, 20.0 mmol) in MeOH (30 mL) was added to the solution. The resulting mixture was concentrated in vacuo, and the residual mass was dispersed in $CHCl_3$ and water. The organic layer was washed with 1.0 M HCl, and saturated NaCl aq., dried over anhydrous $MgSO_4$, and then filtered. The filtrate was concentrated, and the residual mass was purified by recrystallization from $CHCl_3$ and THF to obtain **3** as a brownish solid in 77%. No mp was observed up to 172 °C (decomposition). IR (KBr): 3294, 2096, 1601, 1571, 1433, 1292, 1181, 840, 643, 597 cm^{-1}. ^1H NMR (400 MHz, $CDCl_3$): δ 3.64 (s, 2H, −C≡C*H*), 8.13−8.20 (m, 6H, Ar), 8.61−8.63 (m, 2H, Ar).[51] HRMS. (*m*/*z*): $[M]^+$ calcd for $C_{20}H_{10}$, 250.0783; found, 250.0783.

Polymerization. All the polymerizations were carried out in a glass tube equipped with a three-way stopcock under nitrogen. A typical experimental procedure for polymerization of **1** with **2** is given. A solution of **1** (188 mg, 0.300 mmol), **2** (37.8 mg, 0.300 mmol), $Pd(PPh_3)_2Cl_2$ (10.5 mg, 0.015 mmol), CuI (11.8 mg, 0.045 mmol), PPh_3 (5.70 mg, 0.030 mmol), and Et_3N (1.2 mL) in DMF (1.8 mL) was stirred at 80 °C for 24 h. The resulting mixture was poured into MeOH/acetone [9/1 (v/v), 300 mL] to precipitate the polymer. It was separated by filtration using a membrane filter (ADVANTEC H100A047A) and dried under reduced pressure.

Spectroscopic Data for the Polymers. *Poly[(S)-1−2].* IR (KBr): 3338, 3064, 2925, 2852, 2208, 1735, 1654, 1509, 115, 838, 753, 518 cm^{-1}. ^1H NMR (400 MHz, $CDCl_3$): δ 0.81−0.90 (br, 3H, $-CH_2CH_3$), 1.21−1.34 [br, 21H, $-OCH_2(CH_2)_9-$, $-CH_3$], 1.58−1.73 (br, 2H, $-CH_2CH_3$), 4.10−4.31 [br, 2H, $-OCH_2(CH_2)_9-$], 4.70−4.95 (br, 1H, −C*H*−), 6.50−8.07 (br, 8H, −N*H*−, −O*H*−, Ar).

Poly(1−3a). IR (KBr): 3297, 3058, 2922, 2852, 2211, 1736, 1654, 1509, 1450, 1340, 1205, 1170, 1093, 840, 800, 752, 470 cm^{-1}. ^1H NMR (400 MHz, $CDCl_3$): δ 0.80−0.94 (br, 3H, $-CH_2CH_3$), 1.15−1.34 [br, 21H, $-OCH_2(CH_2)_9-$, $-CH_3$], 1.50−1.69 (br, 2H, $-CH_2CH_3$), 4.21−4.30 [br, 2H, $-OCH_2(CH_2)_9-$], 4.84−4.90 (br, 1H, −C*H*−), 6.46−8.32 (br, 10H, −N*H*−, −O*H*−, Ar).

Poly(1−3b). IR (KBr): 3328, 3058, 2923, 2852, 2200, 1736, 1654, 1509, 1451, 1189, 1161, 1092, 761 cm^{-1}. ^1H NMR (400 MHz, $CDCl_3$): δ 0.80−0.90 (br, 3H, $-CH_2CH_3$), 1.15−1.34 [br, 21H, $-OCH_2(CH_2)_9-$, $-CH_3$], 1.53−1.72 (br, 2H, $-CH_2CH_3$), 4.08−4.31 [br, 2H, $-OCH_2(CH_2)_9-$], 4.78−4.96 (br, 1H, −C*H*−), 6.26−8.60 (br, 10H, −N*H*−, −O*H*−, Ar).

Poly(1−4). IR (KBr): 3423, 3040, 2921, 2851, 2195, 1735, 1654, 1509, 1457, 1341, 1091, 841, 817 cm^{-1}. ^1H NMR (400 MHz, $CDCl_3$): δ 0.72−0.88 (br, 3H, $-CH_2CH_3$), 1.15−1.34 [br, 21H, $-OCH_2(CH_2)_9-$, $-CH_3$], 1.53−1.72 (br, 2H, $-CH_2CH_3$), 4.26−4.41 [br, 2H, $-OCH_2(CH_2)_9-$], 4.83−5.02 (br, 1H, −C*H*−), 6.19−8.87 (br, 12H, −N*H*−, −O*H*−, Ar).

Computation. The MM calculations were carried out using the Merck molecular force field[52] (MMFF94) with Spartan '10 version 1.1.0, running on a Macintosh computer. The ZINDO/S and density functional theory (DFT) calculations were performed with the Gaussian 09 program[53] running on the supercomputer system of the Academic Center for Computing and Media Studies of Kyoto University. The DFT[54] method with Becke's three-parameter hybrid functional[55] and the LYP correlation functional (B3LYP)[56] were utilized in conjunction with the 6-31+G* basis set to fully optimize geometries. Theoretical CD and UV−vis spectra were simulated by the ZINDO/S method[57−61] or by the TD-DFT method. The low-energy transition states of 20 were predicted under the condition of a CI number of 20 × 20, including each oscillator strength (f) and rotatory strength (R_{vel}) in velocity form. The simulated CD and UV−vis spectra were produced by using the R_{vel}− and f−wavelength data with a wavelength-based Gaussian function of 40 nm tentatively used for a half of 1/e-bandwidth.

RESULTS AND DISCUSSION

Polymerization. The Sonogashira−Hagihara coupling polymerization of diiodophenylene monomer **1** with diethynylarylene monomers **2, 3a, 3b**, and **4** was performed in DMF at 80 °C for 24 h to obtain the corresponding polymers [poly(**1**−**2**), poly(**1**−**3a**), poly(**1**−**3b**) and poly(**1**−**4**)] with moderate molecular weights (M_n) in the range 5300−11300 in 88−94% yields (Table 1). The M_n of poly(**1**−**3a**) was relatively low, probably due to the steric hindrance caused by the 2,7-naphthylene linkage. Poly(**1**−**2**), poly(**1**−**3a**) and poly(**1**−**3b**) were soluble in common organic solvents such as CH_2Cl_2, $CHCl_3$, THF, DMSO and DMF. On the other hand, poly(**1**−**4**) was insoluble in CH_2Cl_2, and partly insoluble in $CHCl_3$, DMSO and DMF, likely due to the poor solubility of the rigid pyrene skeleton.

Table 1. Sonogashira−Hagihara Coupling Polymerization of 1 with 2, 3a, 3b and 4[a]

	polymer			
monomer		yield[b] (%)	M_n[c]	M_w/M_n[c]
1 + **2**	poly(**1**−**2**)	90	11300	1.3
1 + **3a**	poly(**1**−**3a**)	94	5300	2.1
1 + **3b**	poly(**1**−**3b**)	88	7500	1.4
1 + **4**	poly(**1**−**4**)	90	11300	1.3

[a]Conditions: $[1]_0 = [2]_0 = [3a]_0 = [3b]_0 = [4]_0$ = 0.10 M, $[Pd(PPh_3)_2Cl_2]$ = 0.0050 M, [CuI] = 0.0025 M, $[PPh_3]$ = 0.0010 M, DMF/Et_3N = 3/2 (v/v), 80 °C, 24 h. [b]Insoluble part in MeOH/acetone =9/1 (v/v). [c]Estimated by SEC measured in THF, polystyrene calibration.

Chiroptical Properties of the Polymers. Figure 1 shows the CD and UV−vis spectra of the polymers measured in THF at 20 °C. Poly(**1**−**3a**), poly(**1**−**2**), poly(**1**−**3b**), and poly(**1**−**4**) exhibited CD signals in the absorption regions of the main chain chromophores around 250−350, 280−400, 300−450 and 350−500 nm, respectively. These CD signals undoubtedly come from the chiral ordered structures of the polymers, since chiral monomer **1** shows the λ_{max} at 286 nm and no CD signal (Figure S1, Supporting Information). The CD and UV−vis

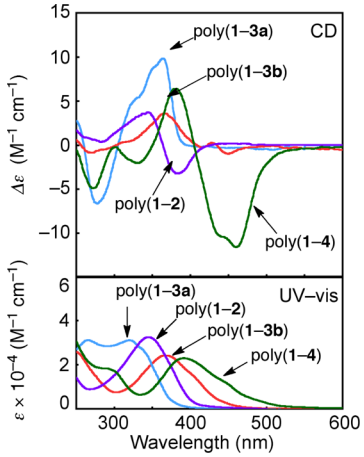

Figure 1. CD and UV−vis spectra of poly(**1**−**2**), poly(**1**−**3a**), poly(**1**−**3b**), and poly(**1**−**4**) measured in THF (c = 30 μM) at 20 °C.

signals were intact after filtering the polymer solutions using a membrane filter with a pore size of 0.45 μm. It is supposed that the CD signals do not originate from chiral aggregation but unimolecular chirality, i.e., folded helical conformations with predominantly one-handed screw sense.[62] The absorption maxima (λ_{max}'s) were remarkably dependent on the arylene units. The λ_{max} of 2,7-naphthylene linked poly(**1**−**3a**) was the shortest (320 nm) among the four polymers, presumably due to the most kinked linkage. The λ_{max}'s of 1,4-naphthylene linked poly(**1**−**3b**) and 1,6-pyrenylene-linked poly(**1**−**4**) were 25 and 50 nm longer than that of poly(**1**−**2**), respectively, indicating the longer conjugation length as predicted from the condensed aromatic rings with the linkages parallel to the main chains.

Figure 2 shows the $\Delta\varepsilon_{max}$ values measured in THF at various temperatures, elucidating the thermal stability of helical

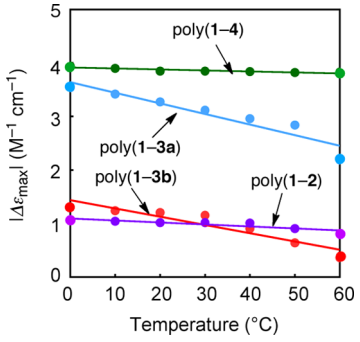

Figure 2. Plot of $|\Delta\varepsilon_{max}|$ value of poly(**1**−**2**), poly(**1**−**3a**), poly(**1**−**3b**), and poly(**1**−**4**) measured in THF (c = 30 μM) at various temperatures.

conformation of the polymers.[63] The $\Delta\varepsilon_{max}$ of poly(**1**−**2**) and poly(**1**−**4**) decreased 24% and 3% by raising temperature from 0 to 60 °C, while those of poly(**1**−**3a**) and poly(**1**−**3b**) decreased 72% and 39%, respectively. The temperature-responsive change was reversible for poly(**1**−**2**) and poly(**1**−**4**), but irreversible for poly(**1**−**3a**) and poly(**1**−**3b**). The stabilities of conformations of the polymers were largely different. The UV−vis signals of poly(**1**−**3a**) and poly(**1**−**3b**) changed upon heating (Figure S2) simultaneously with the CD change. It is likely that the folded helical structures were disrupted, and turned into different structures such as *trans*-zigzag form as increasing the temperature. Once this thermo-induced transformation occurred, refolding into helices seems to be difficult.

The conformation of dynamic helical polymers is largely affected by solvent polarity in most cases, especially when the polymers contain polar functional groups such as amide and hydroxy groups that interact strongly with polar solvents.[1f,h] In the present study, poly(**1**−**4**) exhibited almost the same CD signals in THF/MeOH mixtures irrespective of the composition, although the λ_{max} was slightly blue-shifted as increasing the MeOH content (Figure S3). Poly(**1**−**3a**) exhibited the same trend regarding the solvent effect. On the other hand, the CD signal intensity of poly(**1**−**2**) increased as increasing the MeOH content, while that of poly(**1**−**3b**) decreased. The shape of the UV−vis signals of poly(**1**−**3b**) observed in THF/MeOH = 8/2 mixture almost coincided with that observed at 60 °C in THF. Poly(**1**−**3b**) seems to turn into another structure presumably *trans*-zigzag form not only by heating but also by raising MeOH content. These results indicate that all the polymers are folded into helical structures in THF, and the response to temperature and solvent depends on the structure of arylene unit and linking positions.

It is suggested that poly(**1**−**2**) prefers the left-handed helical structure to the right-handed one from the conformational analysis and simulation of CD spectra.[64] In the present study, the information on the predominance of helical sense of poly(**1**−**3b**) and poly(**1**−**4**) was obtained in a similar fashion. The 24-mers of poly(**1**−**3b**) and poly(**1**−**4**) were constructed with both chain ends terminated with hydrogen atoms. The torsional angles of the main chains were set to −1° and +1° per phenylene unit corresponding to the left- and right-handed helices as the initial geometries. The geometries were optimized by the MM method (MMFF94). The left-handed helical 24-mers of poly(**1**−**3b**) and poly(**1**−**4**) were estimated to be 10.47 and 0.21 kJ/mol•unit more stable than the right-handed counterparts, respectively [Figure S4: the optimized conformers of poly(**1**−**3b**) and poly(**1**−**4**)]. The unimodal and bisignate CD curves were satisfactorily simulated for poly(**1**−**3b**) and poly(**1**−**4**), respectively, by the ZINDO/S method using these conformers (Figure S5). Although the wavelengths were simulated at longer wavelengths than the observed ones, the theoretical CD well supports the predominance of left-handed helical conformers of both poly(**1**−**3b**) and poly(**1**−**4**) in spite of the difference of conjugation units.[65]

Some poly(phenyleneethynylene)s stabilize the helical conformation by intramolecular hydrogen bonds between the pendent groups.[20,21,23,66,67] Solution-state IR spectra of the present polymers were measured together with that of monomer **1** in $CHCl_3$ under diluted conditions (c = 3 mM)[68] to determine the presence/absence of intramolecular hydrogen bonding (Table 2). In every case, a negligibly small

Table 2. Solution-State IR Spectroscopic Data (C═O Absorption Peaks) of Monomer 1 and the Polymers[a]

	wavenumber (cm^{-1}) C═O	
compound	ester	amide
1	1730	1659
poly(**1**−**2**)	1729	1659, 1642
poly(**1**−**3a**)	1731	1652
poly(**1**−**3b**)	1731	1652
poly(**1**−**4**)	1730	1644

[a]Measured in $CHCl_3$ (c = 3 mM).

difference was observed between the wavenumbers of ester C═O absorption peaks of the polymer and **1**. On the other hand, the amide C═O absorption peaks of poly(**1**−**2**), poly(**1**−**3a**), poly(**1**−**3b**) and poly(**1**−**4**) were observed at 7−17 cm^{-1} lower wavenumbers than that of **1**, indicating the presence of intramolecular hydrogen bonds at the amide groups between the side chains in these polymers, and the ester C═O groups do not participate in the hydrogen bonds. Two amide C═O absorption peaks with a ratio of 1:1 were observed in the IR spectrum of poly(**1**−**2**); one was the same wavenumber as that of **1** (1659 cm^{-1}) and the other was 17 cm^{-1} lower. In this case, the amide groups seem to be partly free from hydrogen bonds. This may explain the smallest CD intensity of poly(**1**−**2**) among the polymers as shown in Figure 1. The helical structure of poly(**1**−**2**) appears to be incomplete due to lack of stabilization by intramolecular hydrogen bonds between the amide groups.

dx.doi.org/10.1021/ma401730e | *Macromolecules* 2013, 46, 8896−8904

The fluorescence spectra of the present polymers were measured in THF excited at the main chain based absorption maxima (Figure 3). Poly(**1**−**3a**), poly(**1**−**2**), poly(**1**−**3b**), and

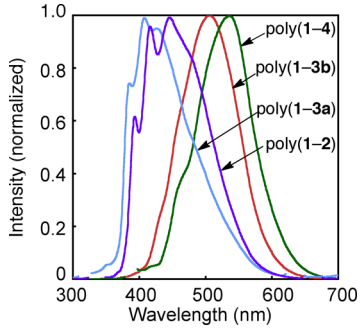

Figure 3. Fluorescence spectra of poly(**1**−**2**), poly(**1**−**3a**), poly(**1**−**3b**), and poly(**1**−**4**) measured in THF (c = 0.6−3.0 μM) at room temperature excited at λ_{max} (342, 320, 367, and 392 nm).

poly(**1**−**4**) emitted purplish blue, blue, green and yellow fluorescence in quantum yields ranging from 18% to 34% (Table 3 and Figure 4).[69] The emission maximum (λ_{emi}) was

Table 3. Optical Data of the Polymers[a]

polymer	λ_{max} (nm)	λ_{emi} (nm)	Φ_{emi}[b] (%)
poly(**1**−**2**)	342	446	31
poly(**1**−**3a**)	320	408	19
poly(**1**−**3b**)	367	504	34
poly(**1**−**4**)	392	535	18

[a]Measured in THF. [b]Measured using anthracene in EtOH (Φ_{emi} = 27%) or quinine sulfate in 0.5 M H_2SO_4 (Φ_{emi} = 54%) as a standard.

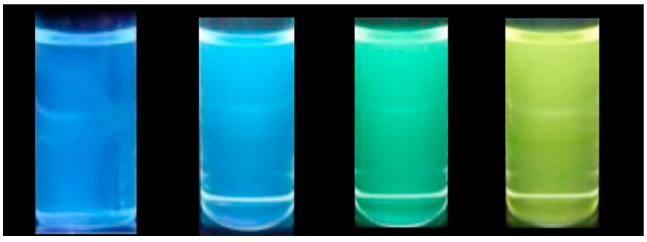

Figure 4. Photograph of THF solutions (c = 3.0 μM) of poly(**1**−**3a**), poly(**1**−**2**), poly(**1**−**3b**), and poly(**1**−**4**) (from left to right) under irradiation of light (365 nm).

red-shifted in consonance with the red-shift of the λ_{max}. Thus, the polymers emitted variously colored fluorescence depending on the arylene units.

Simulation of UV−Vis Spectra. The UV−vis spectra of the model compounds (**M2**, **M3a**, **M3b**, and **M4** in Chart 1) for the polymers were simulated using the TD-DFT method at the B3LYP/6-31+G* level to obtain further information about the conjugation length.[70] Figure 5 depicts the oscillator strength (f) values and UV−vis spectra simulated from the f values and their positions, where a half Gaussian (1/e)-bandwidth (Δ/2) was assumed to be 40 nm.[71] The λ_{max} values were simulated to be 338, 399, 445, and 469 nm for **M3a**, **M2**, **M3b**, and **M4**, respectively, in harmony with the red-shift of observed λ_{max}'s of the polymers as plotted in Figure 6. The most intense f originates from the electron transition from the HOMO to LUMO. The good correlation indicates the properness of TD-DFT calculation on simulating the UV−vis

Chart 1. Structures of Model Compounds

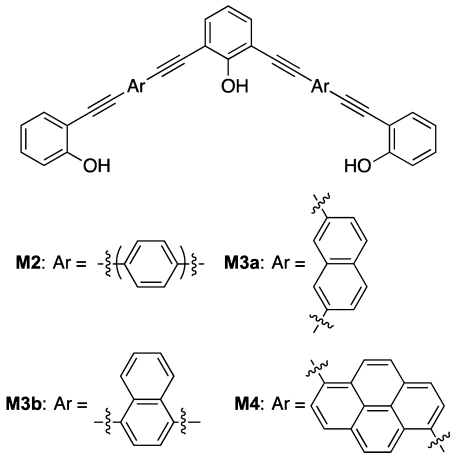

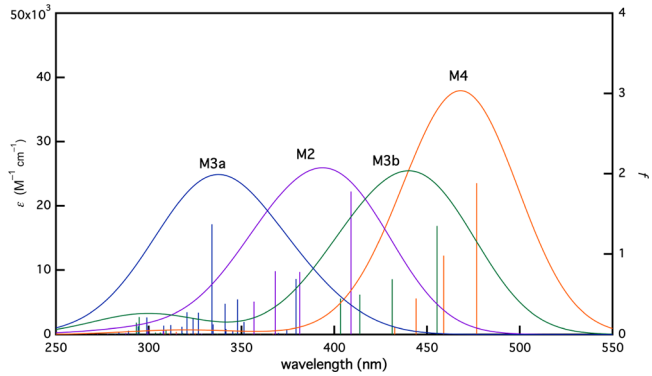

Figure 5. Excited-state parameters and UV−vis spectra simulated for **M2**, **M3a**, **M3b**, and **M4.** The f values (bars) are predicted at the B3LYP/6-31+G* level.

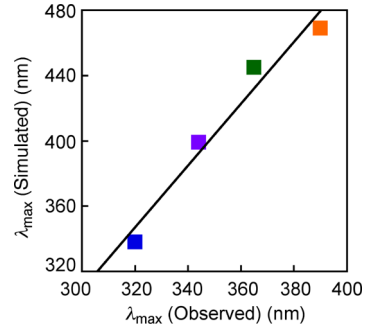

Figure 6. Relationship between the λ_{max} of **M2**, **M3a**, **M3b**, and **M4** simulated at the B3LYP/6-31+G* level and observed λ_{max} of the corresponding polymers [poly(**1**−**2**), poly(**1**−**3a**), poly(**1**−**3b**), and poly(**1**−**4**)]. The data points are colored in accordance with Figure 5.

spectra of phenyleneethynylene polymers. The trend of λ_{max} (**M3a** < **M2** < **M3b** < **M4**) completely agrees with that of HOMO levels of **M2**, **M3a**, **M3b**, and **M4** as listed in Table 4. It appears that the HOMO levels reflect the degree of delocalization of π-electron, which is understood from the shapes of HOMO as illustrated in Figure 7. On the other hand, no clear relation was confirmed between the LUMO levels and λ_{max}.[72]

The experimentally observed λ_{max} values were positioned at shorter wavelengths than those simulated by the TD-DFT method, in a manner similar to several conjugated com-

dx.doi.org/10.1021/ma401730e | Macromolecules 2013, 46, 8896−8904

Table 4. Energy Levels of HOMO and LUMO and Band Gaps (Δ) of Model Compounds M2, M3a, M3b and M4[a]

			Δ	
polymer	HOMO (eV)	LUMO (eV)	(eV)	(nm)
M2	−5.66	−2.25	3.39	366
M3a	−5.81	−2.10	3.71	334
M3b	−5.49	−2.44	3.05	406
M4	−5.07	−2.21	2.86	433

[a]Calculated at the B3LYP/6-31+G* level.

pounds.[73,74] Another possible reason is the degrees of twisting of the main chains. The main chains of the polymers are twisted due to the folded helical structures. On the contrary, the main chains of model compounds **M2**, **M3a**, **M3b**, and **M4** almost exist on a plane to maximize the conjugation. Anyway, we could obtain clear evidence for the effect of arylene structures on the conjugation length of the present polymers based on the TD-DFT calculations.

CONCLUSIONS

In the present study, we have synthesized optically active novel poly(phenyleneethynylene- phenyleneethynylene), poly-(phenyleneethynylene-naphthyleneethynylene)s, and poly-(phenyleneethynylene-pyrenyleneethynylene) bearing hydroxy groups [poly(**1**−**2**), poly(**1**−**3a**), poly(**1**−**3b**), and poly(**1**−**4**)] by the Sonogashira−Hagihara coupling polymerization of optically active diiodophenylene monomer **1** with the corresponding diethynylarylene monomers **2**, **3a**, **3b**, and **4**. CD and UV−vis spectroscopic analysis revealed that all the polymers formed predominantly one-handed folded helical structures in THF. The order of λ_{max} values of the polymers was poly(**1**−**3a**) < poly(**1**−**2**) < poly(**1**−**3b**) < poly(**1**−**4**). It appeared that the 1,4-naphthylene and 1,6-pyrenylene units in the polymer main chains extended the conjugation length compared with phenylene unit, while the 2,7-naphthylene unit rather shortened the conjugation length. Poly(**1**−**2**) and poly(**1**−**4**) formed a thermally stable helical structure in THF, while poly(**1**−**3a**) and poly(**1**−**3b**) lost the regulated helical structures to some extent upon heating. Poly(**1**−**3a**) and poly(**1**−**4**) kept the CD spectroscopic patterns in THF/MeOH irrespective of the MeOH content. On the other hand, poly(**1**−**2**) increased the CD signal intensity upon increasing the MeOH content, while poly(**1**−**3b**) remarkably diminished the CD signals. Namely, the formed polymers showed different temperature- and solvent-responses depending on the arylene

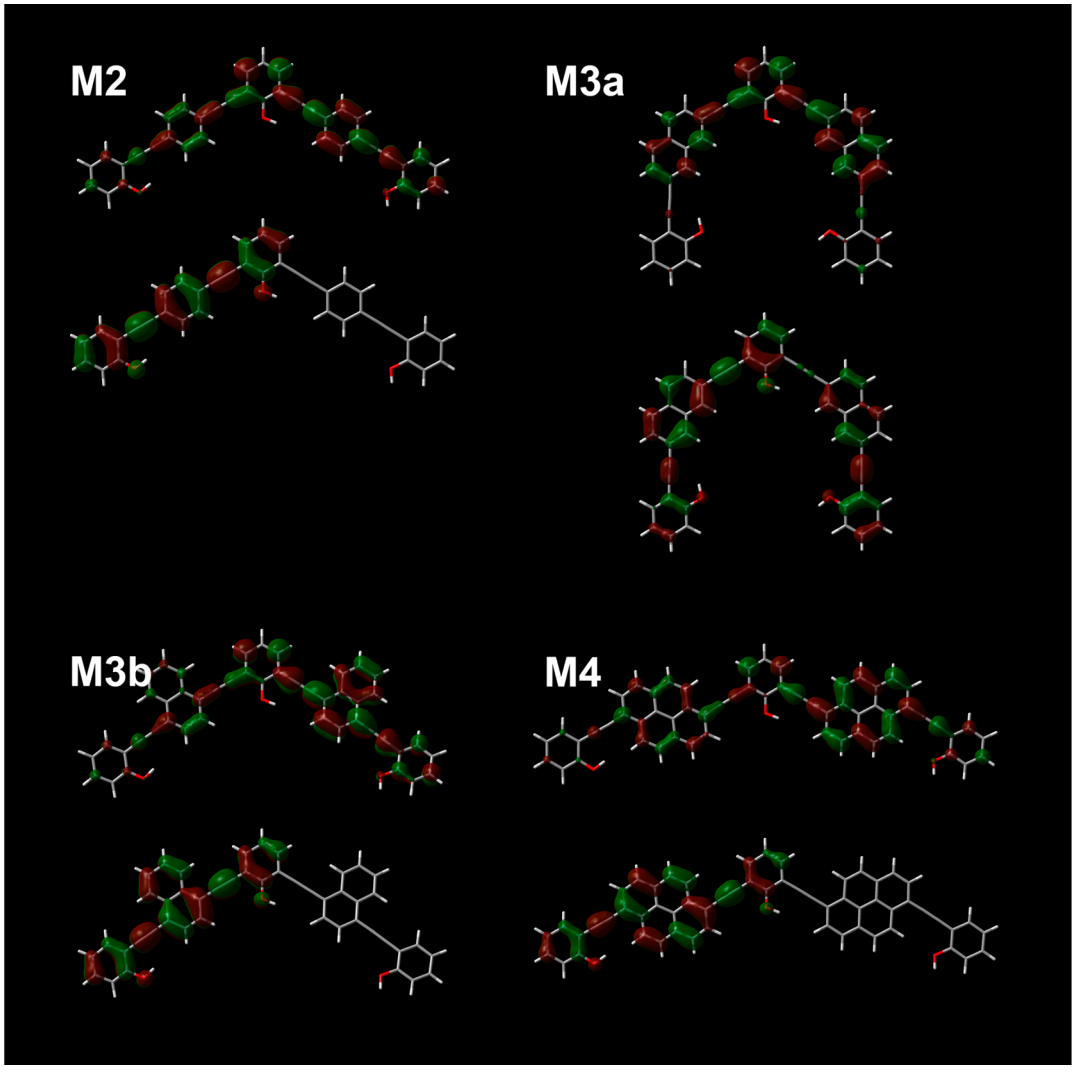

Figure 7. Shapes of HOMO (bottom) and LUMO (top) of **M2**, **M3a**, **M3b**, and **M4** calculated at the B3LYP/6-31+G* level.

dx.doi.org/10.1021/ma401730e | *Macromolecules* 2013, 46, 8896−8904

units and linking positions. The polymers emitted variously colored fluorescence corresponding to the λ_{max}. The TD-DFT simulation for the model compounds of the polymers well agreed with the trend of conjugation length considered by UV–vis spectroscopy. Thus, we could successfully tune the absorption and emission properties of poly(phenyleneethynylene)s by changing the arylene units of diyne monomers. The present study may lead the development of novel sensory or light emissive materials[75,76] as well as establishment of fundamental principles for chemistry of π-conjugated foldamers.

■ ASSOCIATED CONTENT

Supporting Information

CD and UV–vis spectra of monomer **1** measured in THF at 20 °C (Figure S1), poly(**1**–**2**), poly(**1**–**3a**), poly(**1**–**3b**), and poly(**1**–**4**) measured in THF at various temperatures (Figure S2), measured in THF/MeOH mixtures with various compositions at 20 °C (Figure S3), possible conformers of poly(**1**–**3b**) and poly(**1**–**4**) (Figure S4); simulated CD and UV–vis spectra of poly(**1**–**3b**) and poly(**1**–**4**) (Figure S5), photograph of the polymer solutions in THF (Figure S6), structures of achiral and chiral model compounds for UV–vis simulation (Chart S1), simulated UV–vis spectra of achiral and chiral model compounds (Figure S7), transmittance of the polymer solutions measured at 633 nm in THF (Table S1), and Cartesian coordinates of geometries of **M2**, **M3a**, **M3b**, and **M4** optimized at the B3LYP/6-31+G* level. This material is available free of charge via the Internet at http://pubs.acs.org.

■ AUTHOR INFORMATION

Corresponding Author

*E-mail: (F.S.) sanda@kansai-u.ac.jp.

Present Address

[‖](H.S.) Department of Organic and Polymeric Materials, Tokyo Institute of Technology, O-okayama, Meguro-ku, Tokyo 152–8552, Japan

Notes

The authors declare no competing financial interest.

■ ACKNOWLEDGMENTS

This research was supported by JSPS Research Fellowships of Young Scientists and a Grant-in-Aid for Science Research (B) (22350049) from the Japan Society for the Promotion of Science, and by a Grant-in-Aid for Scientific Research on Innovative Areas "New Polymeric Materials Based on Element-Blocks (No. 2401)" from the Ministry of Education, Culture, Sports, Science, and Technology, Japan.

■ REFERENCES

(1) For reviews, see: (a) Choi, S.-K.; Gal, Y.-S.; Jin, S.-H.; Kim, H. K. *Chem. Rev.* **2000**, *100*, 1645–1681. (b) McQuade, D. T.; Pullen, A. E.; Swager, T. M. *Chem. Rev.* **2000**, *100*, 2537–2574. (c) Nagai, K.; Masuda, T.; Nakagawa, T.; Freeman, B. D.; Pinnau, I. *Prog. Polym. Sci.* **2001**, *26*, 721–798. (d) Masuda, T.; Sanda, F. Polymerization of Substituted Acetylenes. In *Handbook of Metathesis*; Grubbs, R. H., Ed., Wiley-VCH, Weinheim, Germany, 2003, Vol. *3*, Chapter 3.11, pp 375–406. (e) Aoki, T.; Kaneko, T.; Teraguchi, M. *Polymer* **2006**, *47*, 4867–4892. (f) Masuda, T. *J. Polym. Sci., Part A: Polym. Chem.* **2007**, *45*, 165–180. (g) Masuda, T.; Sanda, F.; Shiotsuki, M. Polymerization of Acetylenes. In *Comprehensive Organometallic Chemistry III*; Crabtree, R., Mingos, M., Eds., Elsevier, Oxford, U.K., 2007, Vol. *11*, Chapter 16, pp 557–593. (h) Yashima, E.; Maeda, K.; Iida, H.; Furusho, Y.; Nagai, K. *Chem. Rev.* **2009**, *109*, 6102–6211. (i) Akagi, K. *Chem. Rev.* **2009**, *109*, 5354–5401. (j) Liu, J.; Lam, J. W. Y.; Tang, B. Z. *Chem. Rev.* **2009**, *109*, 5799–5867. (k) Masuda, T.; Shiotsuki, M.; Sanda, F. Product Class 31: Macromolecular Conjugated Polyenes. In *Science of Synthesis. Houben-Weyl Methods of Molecular Transformations*, Siegel, J. S.; Tobe, Y., Eds., Georg Thieme Verlag KG: Stuttgart, Germany, and New York, 2010; Category 6, Vol. *45b*, pp 1421–1439. (l) Shiotsuki, M.; Sanda, F.; Masuda, T. *Polym. Chem.* **2011**, *2*, 1044–1058.

(2) For reviews, see: (a) Bunz, U. H. F. *Chem. Rev.* **2000**, *100*, 1605–1644. (b) Egbe, D. A. M.; Carbonnier, B.; Birckner, E.; Grummt, U. *Prog. Polym. Sci.* **2009**, *34*, 1023–1067. (c) Andrew, T. L.; Swager, T. M. *J. Polym. Sci., Part B: Polym. Phys.* **2011**, *49*, 476–498.

(3) Nelson, J. C.; Saven, J. G.; Moore, J. S.; Wolynes, P. G. *Science* **1997**, *277*, 1793–1796.

(4) Prince, R. B; Saven, J. G.; Wolynes, P. G.; Moore, J. S. *J. Am. Chem. Soc.* **1999**, *121*, 3114–3121.

(5) Matsuda, K.; Stone, M. T.; Moore, J. S. *J. Am. Chem. Soc.* **2002**, *124*, 11836–11837.

(6) Arnt, L.; Tew, G. N. *J. Am. Chem. Soc.* **2002**, *124*, 7664–7665.

(7) Abe, H.; Masuda, N.; Waki, M.; Inouye, M. *J. Am. Chem. Soc.* **2005**, *127*, 16189–16196.

(8) Jones, T. V.; Slutsky, M. M.; Laos, R.; Greef, T. F. A.; Tew, G. N. *J. Am. Chem. Soc.* **2005**, *127*, 17235–17240.

(9) Khan, A.; Hecht, S. *Chem.—Eur. J.* **2006**, *12*, 4764–4774.

(10) Wackerly, J. W.; Moore, J. S. *Macromolecules* **2006**, *39*, 7269–7276.

(11) Zhao, X.; Schanze, K. S. *Langmuir* **2006**, *22*, 4856–4862.

(12) Smaldone, R. A.; Moore, J. S. *J. Am. Chem. Soc.* **2007**, *129*, 5444–5450.

(13) Zhu, M.; Lu, W.; Zhu, N.; Che, C. *Chem.—Eur. J.* **2008**, *14*, 9736–9746.

(14) Block, M. A. B.; Hecht, S. *Macromolecules* **2008**, *41*, 3219–3227.

(15) Zhu, N.; Hu, W.; Han, S.; Wang, Q.; Zhao, D. *Org. Lett.* **2008**, *10*, 4283–4286.

(16) Inoue, M.; Teraguchi, M.; Aoki, T.; Hadano, S.; Namikoshi, T.; Marwanta, E.; Kaneko, T. *Synth. Mater.* **2009**, *159*, 854–858.

(17) Zhang, Z.; Che, Y.; Smaldone, R. A.; Xu, M.; Bunes, B. R.; Moore, J. S.; Zang, L. *J. Am. Chem. Soc.* **2010**, *132*, 14113–14117.

(18) Jiang, J.; Slutsky, M. M.; Jones, T. V.; Tew, G. N. *New J. Chem.* **2010**, *34*, 307–312.

(19) Chen, Y.; Malkovskiy, A.; Wang, X.; Lebron-Colon, M.; Sokolov, A. P.; Perry, K.; More, K.; Pang, Y. *ACS Macro Lett.* **2012**, *1*, 246–251.

(20) Banno, M.; Yamaguchi, T.; Nagai, K.; Kaiser, C.; Hecht, S.; Yashima, E. *J. Am. Chem. Soc.* **2012**, *134*, 8718–8728.

(21) Liu, R.; Shiotsuki, M.; Masuda, T.; Sanda, F. *Macromolecules* **2009**, *42*, 6115–6122.

(22) Liu, R.; Sogawa, H.; Shiotsuki, M.; Masuda, T.; Sanda, F. *Polymer* **2010**, *51*, 2255–2263.

(23) Sogawa, H.; Shiotsuki, M.; Matsuoka, H.; Sanda, F. *Macromolecules* **2011**, *44*, 3338–3345.

(24) Hashimoto, A.; Sogawa, H.; Shiotsuki, M.; Sanda, F. *Polymer* **2012**, *53*, 2559–2566.

(25) Sogawa, H.; Shiotsuki, M.; Sanda, F. *Macromolecules* **2013**, *46*, 4378–4387.

(26) Shizuka, H. *Pure Appl. Chem.* **1997**, *69*, 825–830.

(27) Yang, F.; Akhtaruzzaman, M.; Islam, A.; Jin, T.; El-Shafei, A.; Qin, C.; Han, L.; Alamry, K. A.; Kosa, S. A.; Hussein, M. A.; Asiri, A. M.; Yamamoto, Y. *J. Mater. Chem.* **2012**, *22*, 22550–22557.

(28) Winnilk, F. M. *Chem. Rev.* **1993**, *93*, 587–614.

(29) Karuppannan, S.; Chambron, J. *Chem. Asian J.* **2011**, *6*, 964–984.

(30) Zhou, C.; Wang, W.; Lin, K. K.; Chen, Z.; Lai, Y. *Polymer* **2004**, *45*, 2271–2279.

(31) Kijima, M.; Mori, T. *Opt. Mater.* **2007**, *30*, 545–552.

(32) Zhao, Z.; Xu, X.; Jiang, Z.; Lu, P.; Yu, G.; Liu, Y. *J. Org. Chem.* **2007**, *72*, 8345–8353.

(33) Chen, H.; Hu, X.; Ng, S. *J. Polym. Sci., Part A: Polym. Chem.* **2010**, *48*, 5562–5569.

(34) Gupta, J.; Vadukumpully, S.; Valiyaveettil. *Polymer* **2010**, *51*, 5078−5086.
(35) He, G.; Yan, N.; Yang, J.; Wang, H.; Ding, L.; Yin, S.; Fang, Y. *Macromolecules* **2011**, *44*, 4759−4766.
(36) Shen, D.; Diele, S.; Pelzl, G.; Wirth, I.; Tschierske, C. *J. Mater. Chem.* **1999**, *9*, 661−672.
(37) Nomura, R.; Yamda, K.; Masuda, T. *Chem. Commun.* **2002**, 478−479.
(38) Zhao, H.; Sanda, F.; Masuda, T. *Macromolecules* **2004**, *37*, 8893−8896.
(39) Zhao, H.; Sanda, F.; Masuda, T. *Polymer* **2006**, *47*, 1584−1589.
(40) Yuan, W. Z.; Sun, J. Z.; Dong, Y.; Häussler, M.; Yang, F.; Xu, H. P.; Qin, A.; Lam, J. W. Y.; Zhen, Q.; Tang, B. Z. *Macromolecules* **2006**, *39*, 8011−8020.
(41) Lin, H.; Morino, K.; Yashima, E. *Chirality* **2008**, *20*, 386−392.
(42) Sogawa, H.; Shiotsuki, M.; Sanda, F. *J. Polym. Sci., Part A: Polym. Chem.* **2012**, *50*, 2008−2018.
(43) Ishiwari, F.; Nakazono, K.; Koyama, Y.; Takata, T. *Chem. Commun.* **2011**, *47*, 11739−11741.
(44) Kakuchi, R.; Nagata, S.; Sakai, R.; Otsuka, I.; Nakade, H.; Satoh, T.; Kakuchi, T. *Chem.—Eur. J.* **2008**, *14*, 10259−10266.
(45) Kakuchi, R.; Kodama, T.; Shimada, R.; Tago, Y.; Sakai, R.; Satoh, T.; Kakuchi, T. *Macromolecules* **2009**, *42*, 3892−3897.
(46) Yashima, E.; Maeda, K.; Sato, O. *J. Am. Chem. Soc.* **2001**, *123*, 8159−8160.
(47) Ma, L.; Hu, Q.; Pu, L. *Tetrahedron: Assym.* **1996**, *7*, 3103−3106.
(48) Gómez, R.; Segura, J. L.; Martín, N. *J. Org. Chem.* **2000**, *65*, 7501−7511.
(49) Neenan, T. X.; Whitesides, G. M. *J. Org. Chem.* **1988**, *53*, 2489−2496.
(50) Khan, M. S.; Al-Mandhary, M. R. A.; Al-Suti, M. K.; Al-Battashi, F. R.; Al-Saadi, S.; Ahrens, B.; Bjernemose, J. K.; Mahon, M. F.; Raithby, P. R.; Younus, M.; Chawdhury, N.; Köhler, A.; Marseglia, E. A.; Tedesco, E.; Feeder, N.; Teat, S. J. *Dalton Trans.* **2004**, 2377−2385.
(51) Ji, S.; Yang, J.; Yang, Q.; Liu, S.; Chen, M.; Zhao, J. *J. Org. Chem.* **2009**, *74*, 4855−4865.
(52) Halgren, T. A. *J. Comput. Chem.* **1996**, *17*, 490−519 The MM calculations were carried out with *Wavefunction, Inc., Spartan '10 Macintosh*..
(53) Frisch, M. J.; Trucks, G. W.; Schlegel,H. B.; Scuseria, G. E.; Robb, M. A.; Cheeseman, J. R.; Scalmani, G.; Barone, V.; Mennucci, B.; Petersson, G. A.; Nakatsuji, H.; Caricato, M.; Li, X.; Hratchian, H. P; Izmaylov, A. F.; Bloino, J.; Zheng, G.; Sonnenberg, J. L.; Hada, M.; Ehara, M.; Toyota, K.; Fukuda, R.; Hasegawa, J.; Ishida, M.; Nakajima, T.; Honda, Y.; Kitao, O.; Nakai, H.; Vreven, T.; Montgomery, J. A.; Peralta, Jr., J. E.; Ogliaro, F.; Bearpark, M.; Heyd, J. J.; Brothers, E.; Kudin, K. N.; Staroverov, V. N.; Keith,T.; Kobayashi, R.; Normand, J.; Raghavachari, K.; Rendell, A.; Burant, J. C.; Iyengar, S. S.; Tomasi, J.; Cossi, M.; Rega, N.; Millam, J. M.; Klene, M.; Knox, J. E.; Cross, J. B.; Bakken, V.; Adamo, C.; Jaramillo, J.; Gomperts, R.; Stratmann, R. E.; Yazyev, O.; Austin, A. J.; Cammi, R.; Pomelli, C.; Ochterski, J. W.; Martin, R. L.; Morokuma, K.; Zakrzewski, V. G.; Voth, G. A.; Salvador, P.; Dannenberg, J. J.; Dapprich, S.; Daniels, A. D.; Farkas, O.; Foresman, J. B.; Ortiz, J. V.; Cioslowski, J.; Fox, D. J. *Gaussian 09, Revision B.01*; Gaussian, Inc.: Wallingford, CT, 2010.
(54) Parr, R. G.; Yang, W. *Density-Functional Theory of Atoms and Molecules*; Oxford University Press: Oxford, U.K., 1989.
(55) Becke, A. D. *J. Chem. Phys.* **1993**, *98*, 5648−5652.
(56) Lee, C. T.; Yang, W. T.; Parr, R. G. *Phys. Rev. B* **1988**, *37*, 785−789.
(57) Ridley, J. E.; Zerner, M. C. *Theor. Chem. Acc.* **1973**, *32*, 111−134.
(58) Ridley, J. E.; Zerner, M. C. *Theor. Chem. Acc.* **1976**, *42*, 223−236.
(59) Bacon, A. D.; Zerner, M. C. *Theor. Chem. Acc.* **1979**, *53*, 21−54.
(60) Zerner, M. C.; Loew, G. H.; Kirchner, R. F.; Mueller-Westerhoff, U. T. *J. Am. Chem. Soc.* **1980**, *102*, 589−599.
(61) Thompson, M. A.; Zerner, M. C. *J. Am. Chem. Soc.* **1991**, *113*, 8210−8215.
(62) It has been reported that membrane filtration of solutions of conjugated polymers is effective to remove aggregates. See: Yamamoto, T.; Komarudin, D.; Arai, M.; Lee, B.-L.; Suganuma, H.; Asakawa, N.; Inoue, Y.; Kubota, K.; Sasaki, S.; Fukuda, T.; Matsuda, H. *J. Am. Chem. Soc.* **1998**, *120*, 2047−2058.
(63) The Kuhn dissymmetry factor ($g = \Delta\varepsilon/\varepsilon$) gives quantitative information associated with the degree of preferential screw sense. In the present study however, the peak top wavelengths of UV−vis signals of the polymers largely changed upon heating probably due to the helix-random transition, which made the *g*-based discussion on enantiomeric excess of helical conformation difficult. We therefore plotted $\Delta\varepsilon$−temperature relationships in Figure 2 to discuss the temperature-dependent conformational changes of the polymers. Representative papers regarding *g*, see (a) Kuhn, W. *Trans. Faraday Soc.* **1930**, *26*, 239−308. (b) Fujiki, M. *Macromol. Rapid Commun.* **2001**, *22*, 539−563.
(64) Sogawa, H.; Shiotsuki, M.; Hirao, T.; Haino, T.; Sanda, F. *Macromolecules* **2013**, DOI: 10.1021/ma4017295.
(65) The conformation analysis of poly(**1**−**3a**) was not carried out because of the presence of many possible conformers according to the directions of the 1,4-naphthylene groups, which makes the conformation analysis difficult.
(66) Cary, J. M.; Moore, J. S. *Org. Lett.* **2002**, *4*, 4663−4666.
(67) Yang, X.; Brown, A. L.; Furukawa, M.; Li, S.; Gardinier, W. E.; Bukowski, E. J.; Bright, F. V.; Zheng, C.; Zeng, X. C.; Gong, B. *Chem. Commun.* **2003**, 56−57.
(68) This concentration is sufficiently low to eliminate the effect of intermolecular hydrogen bonding. See Silverstein, R. M.; Webster, F. X.; Kiemle, D. J. Infrared Spectrometry. In *Spectrometric Identification of Organic Compounds*, 7th ed.; John Wiley & Sons: New York, 2005; Chapter 2. It is confirmed that all the polymers show almost the same CD spectra in THF and $CHCl_3$.
(69) Although the sample solutions under UV light shown in Figure 4 look a little bit turbid, the solutions are highly transparent as shown in the photograph under visible light (Figure S6). The transmittance of the polymer solutions in THF at 633 nm was almost 100% in all cases (Table S1). It is likely that the unimolecular polymer exhibited the chiroptical property by forming a folded helical structure, not by aggregation.
(70) The UV−vis spectra of model compounds with chiral substituents were also simulated in a similar fashion. The chiral model compounds are predicted to exhibit almost the same λ_{max} values as those of the achiral ones (Chart S1 and Figure S7).
(71) In all cases, a half Gaussian (1/e)-bandwidth ($\Delta/2$) was assumed to be 40 nm. The simulated UV−vis spectra are sensitive to ($\Delta/2$) value. We employed this value because it yielded absorption profiles that visually reflected experimental ones, as a result, although it was a little bit large. About ($\Delta/2$) dependence of simulated spectra, see Komori, H.; Inai, Y. *J. Phys. Chem. A* **2006**, *110*, 9099−9107.
(72) The LUMO level of **M3a** is the highest and the HOMO level of **M3a** is the lowest among those of the four model compounds, resulting in the largest band gap (3.71 eV, 334 nm). As mentioned in the main text, the conjugation becomes long and λ_{max} is red-shifted as the HOMO level becomes high. The HOMO level of **M3b** is higher than that of **M3a**, and the LUMO level of **M3b** is lower than that of **M3a**, resulting in the smaller band gap (3.05 eV, 406 nm). Consequently, **M3a** and **M3b** possessed such different λ_{max} values. One of the reviewers pointed out that the LUMOs of four model compounds are delocalized along the main chain, but the HOMOs of **M2**, **M3a**, and **M4** are localized at a half side of the respective main chain, while the HOMO of **M3b** is delocalized whole of the main chain. At the moment, we cannot clearly explain the reason for the difference of the HOMO shapes between **M3b** and the other model compounds.
(73) Nguyen, K. A.; Rogers, J. E.; Slagle, J. E.; Day, P. N.; Kannan, R.; Tan, L.-S.; Fleitz, P. A.; Pachter, R. *J. Phys. Chem. A* **2006**, *110*, 13172−13182.

(74) Jungsuttiwong, S.; Tarsang, R.; Surakhot, Y.; Khunchalee, J.; Sudyoadsuk, T.; Promarak, V.; Namuangruk, S. *Org. Electron.* **2012**, *13*, 1836−1843.
(75) Zhao, X.; Pinto, M. R.; Hardison, R. P.; Hardison, L. M.; Mwaura, J.; Muller, J.; Jiang, H.; Witker, D.; Kleiman, V. D.; Reynolds, J. R.; Schanze, K. S. *Macromolecules* **2006**, *39*, 6355−6366.
(76) Tanaka, K.; Chujo, Y. *Macromol. Rapid Commun.* **2012**, *33*, 1235−1255.